

# Fiber oscillator of 5 kW using fiber Bragg gratings inscribed by a visible femtosecond laser

Hongye Li (李宏业)<sup>1,2</sup>, Xin Tian (田鑫)<sup>1,2</sup>, Hao Li (李昊)<sup>1,2</sup>, Baiyi Wu (武柏屹)<sup>1,2</sup>, Xiaofan Zhao (赵晓帆)<sup>1,3</sup>, Meng Wang (王蒙)<sup>1,2,3</sup>, Chenhui Gao (高晨晖)<sup>1,3</sup>, Binyu Rao (饶斌裕)<sup>1</sup>, Xiaoming Xi (奚小明)<sup>1</sup>, Zilun Chen (陈子伦)<sup>1</sup>, Zefeng Wang (王泽锋)<sup>1,2,3\*</sup>, and Jinbao Chen (陈金宝)<sup>1</sup>

<sup>1</sup> College of Advanced Interdisciplinary Studies, National University of Defense Technology, Changsha 410073, China

<sup>2</sup> State Key Laboratory of Pulsed Power Laser Technology, Changsha 410073, China

<sup>3</sup> Hunan Provincial Key Laboratory of High Energy Laser Technology, Changsha 410073, China

\*Corresponding author: [hotrosemaths@163.com](mailto:hotrosemaths@163.com)

Received May 30, 2022 | Accepted August 15, 2022 | Posted Online September 16, 2022

We fabricate a pair of fiber Bragg gratings (FBGs) by a visible femtosecond laser phase mask scanning technique on passive large-mode-area double-cladding fibers for multi-kilowatt fiber oscillators. The bandwidth of high-reflection (HR) and low-reflection (LR) FBG is  $\sim 1.6$  nm and 0.3 nm, respectively. The reflection of the HR-FBG is higher than 99%, and that of the LR-FBG is about 10%. A bidirectional pumped all-fiber oscillator is constructed using this pair of FBGs, a record output power of 5027 W located in the signal core is achieved with a slope efficiency of  $\sim 82.1\%$ , and the beam quality factor  $M^2$  is measured to be  $\sim 1.6$  at the maximum power. The FBGs are simply fixed on a water cooling plate without a special package, and the thermal efficiency of the HR-FBG and the LR-FBG is  $2.76^\circ\text{C}/\text{kW}$  and  $1^\circ\text{C}/\text{kW}$ , respectively. Our research provides an effective solution for robust high-power all-fiber laser oscillators.

**Keywords:** fiber optics; fiber lasers; fiber Bragg gratings.

**DOI:** [10.3788/COL202321.021404](https://doi.org/10.3788/COL202321.021404)

## 1. Introduction

High-power all-fiber lasers have largely been utilized in industry, scientific research, and defense technology for their high efficiency, good beam quality, and robustness<sup>[1,2]</sup>. In general, two structures, namely amplifiers and oscillators, are employed to achieve kilowatt (kW)-level fiber lasers. In recent years, benefiting from the large-mode-area (LMA) fiber Bragg gratings (FBGs) fabrication technique, the all-fiber oscillator structure (which is not amplified) has gradually replaced the role of the master oscillator power amplifier (MOPA) structure in many applications<sup>[3–13]</sup>. Compared with MOPA, the oscillator has a more compact structure, higher resistance to back-propagating light, and simpler operation. The first, to the best of our knowledge, all-fiber kW-level oscillator was reported by Alflight company in 2012<sup>[4]</sup>. After that, the output power of the all-fiber oscillator scaled up step-by-step. The National University of Defense Technology and Fujikura company reported single mode 3 kW all-fiber oscillators in 2017<sup>[7,8]</sup>. Then, the maximum output power scaled up to the 5 kW level in 2018<sup>[9,10]</sup>. All-fiber oscillators at the 6 kW level were also realized by suppressing transverse mode instability (TMI) or stimulated Raman scattering (SRS) effects<sup>[11,12]</sup>. In 2020, Fujikura company realized an

8 kW single mode oscillator using their home-made ytterbium-doped fibers (YDFs) and FBGs<sup>[13]</sup>, which is the maximum output power so far.

FBGs are indispensable devices in all-fiber oscillators, which play the role of reflector and output coupler. Investigations showed that the FBG could influence the threshold of the SRS effect<sup>[14]</sup> and the TMI effect<sup>[15]</sup>. Thus, the output power of the oscillator is directly decided by the quality of FBGs. Ultraviolet (UV) exposure<sup>[16]</sup> is the most common method to fabricate FBGs used in oscillators. Hydrogen loading is an irrevocable process before FBG is fabricated by the UV exposure method. After inscription, thermal annealing should be carried out to remove hydrogen in the fibers. However, only constant high temperature is not enough. Stepped heating and cooling is selected by researchers to reduce hydroxyl concentration in the FBGs<sup>[17]</sup>. In spite of this, the yield rate of FBGs is still very low, and the whole fabrication process is time-consuming. The femtosecond laser is regarded as a promising alternative to the UV exposure method<sup>[18]</sup>. Photosensitivity is not necessary, and thus hydrogen loading and thermal annealing can be neglected. The femtosecond laser direct writing technique<sup>[19,20]</sup> has proven its value in inscribing FBGs used in sensing applications, but, owing to their unavoidable insertion loss<sup>[21,22]</sup>, the FBGs fabricated by

this method cannot apply in high-power lasers. The femtosecond laser phase mask technique is a potential way to fabricate FBGs for high-power fiber oscillators. In 2019, Krämer *et al.* realized a 1.9 kW fiber oscillator by inscribing a high-reflection (HR) FBG on an LMA-YDF (with core/inner-cladding diameter of 20/400  $\mu\text{m}$ ) using the infrared (IR) femtosecond laser phase mask scanning technique<sup>[23]</sup>, and then a 5 kW oscillator was constructed by using a pair of FBGs in passive fibers<sup>[24]</sup>. Except these two investigations, we realized a 3.2 kW all-fiber oscillator using a pair of FBGs inscribed by a visible femtosecond laser<sup>[25]</sup>. The inscription process and the characteristics of the FBG inscribed by the femtosecond laser should be studied in detail to find out the best solution for this issue.

In this Letter, we explore the inscription of LMA-FBGs (with a core/inner-cladding diameter of 20/400  $\mu\text{m}$ ) using the visible femtosecond laser phase mask scanning technique. An all-fiber oscillator is established using a pair of FBGs fabricated by a visible femtosecond laser. The maximum output power is 5027 W, with a slope efficiency of 82.1%, and the beam quality factor ( $M^2$ ) at the maximum power is 1.6. The thermal efficiency of the HR-FBG and low-reflection (LR) FBG is 2.76°C/kW and 1°C/kW, respectively. We realize the record output power of the oscillator by femtosecond laser inscribed FBGs with a core/inner-cladding diameter of 20/400  $\mu\text{m}$ . The research provides a solution for robust high-power all-fiber oscillators.

## 2. FBG and High-Power Oscillator

Figure 1(a) indicates the schematic of the femtosecond laser phase mask scanning method. The wavelength of femtosecond laser is 515 nm, the repetition rate is 1 kHz, the pulse duration is

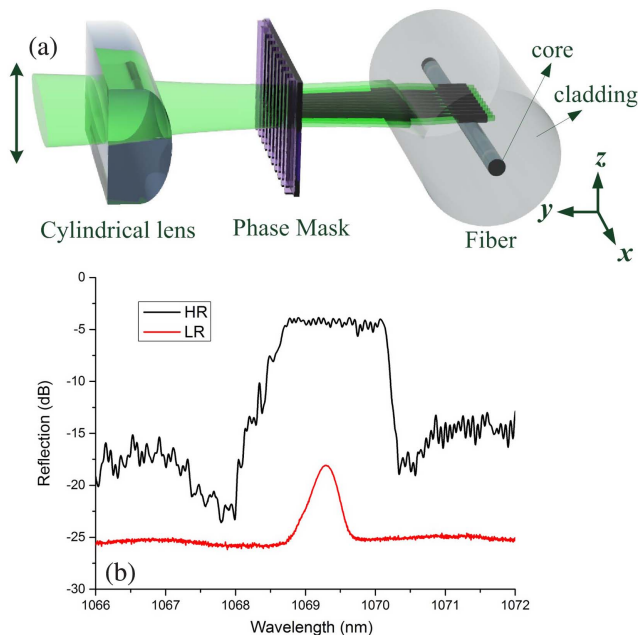


Fig. 1. (a) Schematic of the femtosecond laser phase scanning method. (b) Reflection spectra of HR-FBG and LR-FBG.

190 fs, and the pulse energy is 255  $\mu\text{J}$ . For the visible femtosecond laser, the alignment process before inscription is simpler than the invisible counterpart. Moreover, the diffraction limit of visible light is smaller than that of invisible light, and thus the pulse energy for FBG inscription can be decreased. Before reaching the phase mask, the femtosecond laser passes through a cylindrical lens with focal length of 25 mm to compress the size of the beam in the  $z$  direction. The average pitch of the phase mask is 1473.8 nm, and the chirped rate is 0.5 nm/cm. The fiber is set near the focus, and the distance between the fiber and phase mask is longer than 1 mm. This allows us to avoid interference with the zeroth-order diffracted beam by the walk-off effect<sup>[26]</sup>. As the beam diameter is only 3 mm, the laser beam should be moved along the  $x$  direction (fiber axis) to realize the inscription of FBGs with a length longer than 1 cm. Besides, larger refractive index modulation can be achieved by vibrating the laser beam in the  $z$  direction (vertical to the fiber axis). Figure 1(b) is the reflection spectra of HR-FBG and LR-FBG. The FBGs are inscribed with stripped polymer coating, and the fiber is recoated with a coating machine after inscription. The length of HR-FBG is 4 cm, the reflection is higher than 99%, the central wavelength is 1069.4 nm, and the 3 dB bandwidth is  $\sim 1.6$  nm. The length of LR-FBG is only 3 mm, which is inscribed by only vibrating the laser beam in the  $z$  direction, the reflection is about 10%, the Bragg wavelength is 1069.3 nm, and the bandwidth is  $\sim 0.3$  nm.

Figure 2 shows the setup of the high-power all-fiber oscillator. The bidirectional pump scheme is carried out in our experiment. The length of YDFs (Coherent YDF 20/400) is  $\sim 19$  m, and the absorption coefficient is  $\sim 1.26$  dB/m at 976 nm. The YDFs are coiled in circles, and the diameter of the circles varies from  $\sim 8.5$  cm to  $\sim 12.5$  cm. The pump-signal combiners are spliced to both ends of the YDF. Six pump ports and one signal port constitute a combiner. The core/inner cladding diameter of the pump port is 220/242  $\mu\text{m}$ , and that of the signal port is 20/400  $\mu\text{m}$ . Two pump ports in the forward combiner and all the pump ports in the backward combiner are spliced with 976 nm laser diodes (LDs) with its maximum power  $\sim 900$  W. Two combiners and YDFs are set between HR-FBG and LR-FBG. In order to suppress the influence of facet reflection, two quartz block heads (QBHs) are spliced with HR-FBG and LR-FBG, respectively. A cladding light stripper (CLS) is utilized to remove the residual pump light before laser output. All the components including YDFs, combiners, FBGs, and CLSs are placed on a water cooling plate. What has to be pointed out is that no special package is exerted on HR-FBG and LR-FBG to facilitate temperature monitoring during the power scaling process.

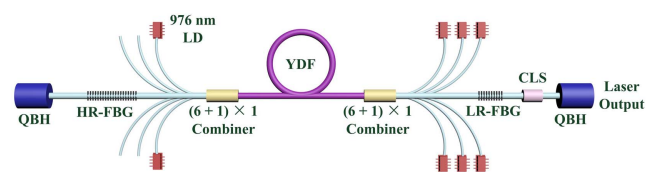


Fig. 2. Schematic of the high-power fiber oscillator.

### 3. Experimental Results

Figure 3 shows the relationship between output power and pump power. During experiment, the counter-pump power is firstly injected into the oscillator, and then the co-pump power is. When the counter-pump power reaches its maximum value at 5551 W, the output power is 4528 W. After that, we add co-pump power to 600 W, and the output power increases to 5027 W. The slope efficiency of the oscillator is 82.1%. No roll-over output power or laser efficiency is observed during the power scaling process. Moreover, in order to monitor the occurrence of TMI, we record the temporal domain signal using a photodetector, and no fluctuation occurs at the operation of 5027 W. Thus, the TMI effect does not appear in the power scaling process. The insets in Fig. 3 indicate the beam profile under different output power. The beam quality factor ( $M^2$ ) is around 1.5 when the output power is lower than 4528 W. When the output power reaches 5027 W, the beam quality factor deteriorates to 1.6.

Laser spectra under different output power are illustrated in Fig. 4. The full width at half-maximum (FWHM) of the laser broadens with the power scaling as a result of the fiber nonlinear effect like self-phase modulation (SPM). The FWHM at the operation of 3005 W is  $\sim 4.6$  nm, and this value increases to  $\sim 7.2$  nm when the output power ascends to 5072 W. The central wavelength of the laser is  $\sim 1069.7$  nm, which is slightly larger than the Bragg wavelength of LR-FBG. As the LR-FBG endures all the output power, the heat load cannot be ignored in the high-power environment, and thus the resonant point of LR-FBG shifts to a longer wavelength. Besides, Raman-Stokes light occurs near  $\sim 1124$  nm when the output power is higher than 3005 W, and the intensity of the SRS effect goes up dramatically with power scaling. The intensity of Raman-Stokes light is 18 dB below the laser intensity when the output power reaches 5027 W. Limited by the SRS effect, the output power cannot be further scaled up. A larger modal area fiber is a solution for this issue.

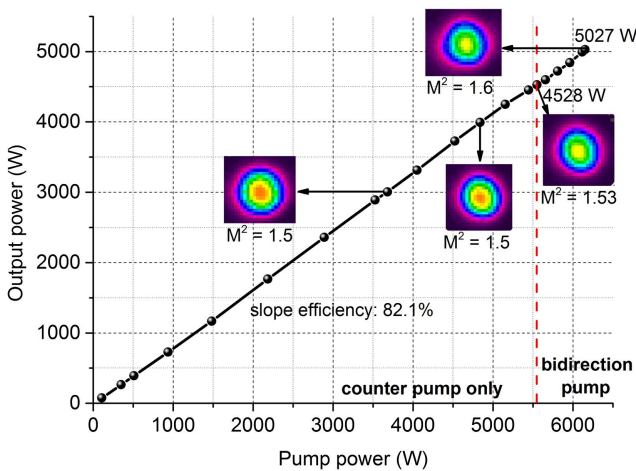


Fig. 3. Output power versus pump power. Insets: beam profiles at the operation of 3005 W, 3992 W, 4528 W, and 5027 W.

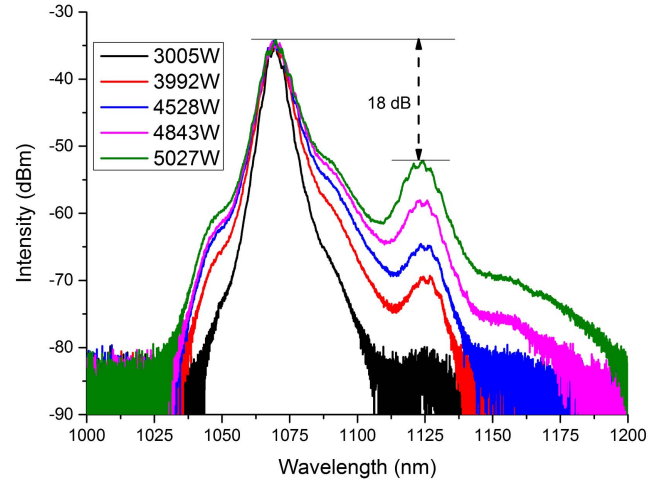


Fig. 4. Laser spectra under different output power.

Thermal behavior of FBGs is the most critical issue when assessing the durability of high-power oscillators. For FBGs fabricated by the UV exposure method, if hydrogen is not expelled

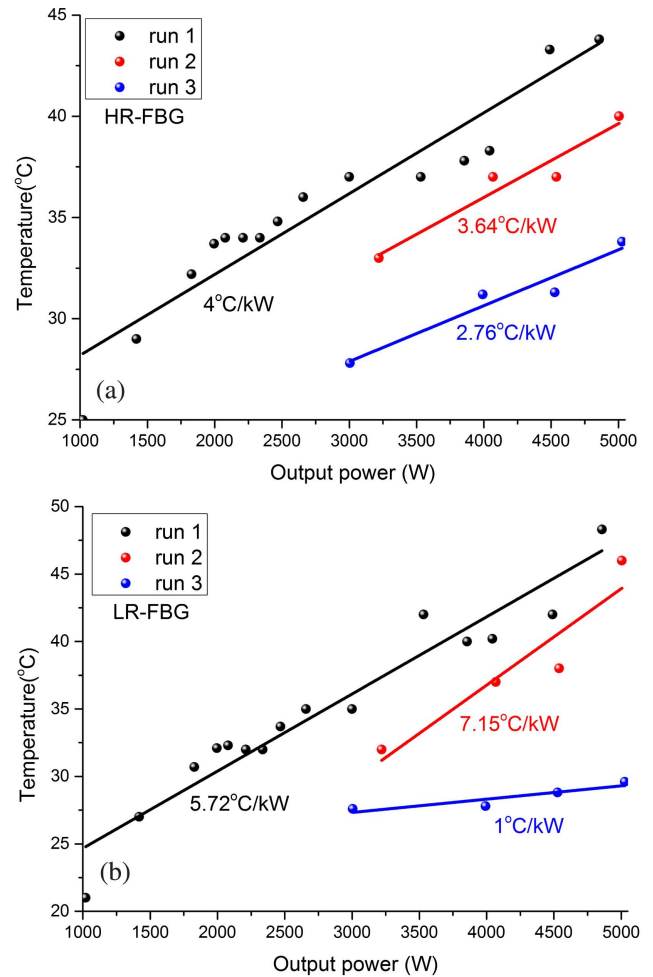
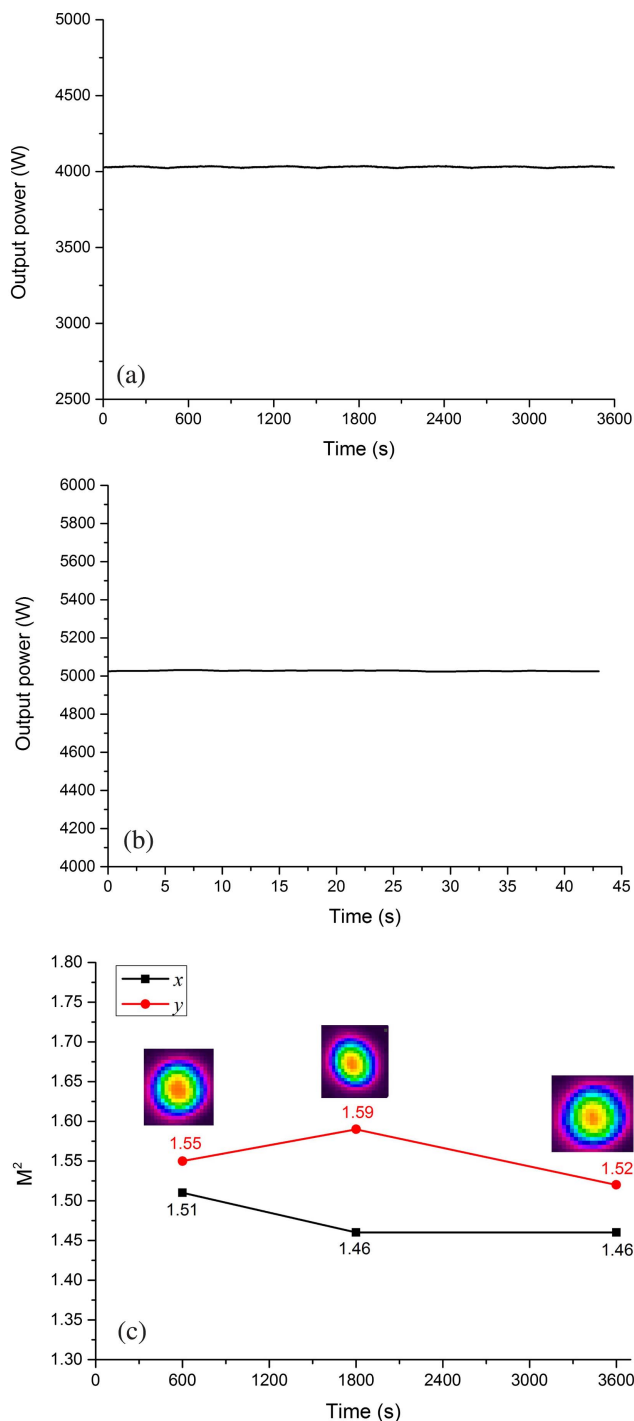


Fig. 5. Temperature of (a) HR-FBG and (b) LR-FBG at different operation power.

completely during thermal annealing, the temperature of FBGs grows up dramatically with the output power. Figure 5 demonstrates the temperature shift of HR-FBG and LR-FBG at different operation power. We record the temperature of FBGs within three runs of the laser experiment via an IR camera. The temperature of HR-FBG and LR-FBG increases with the operation



**Fig. 6.** Oscillator stability test: (a) variation of output power at the operation of  $\sim 4030$  W during 1 h, (b) variation of output power at the operation of 5027 W, and (c) variation of beam quality measured at  $\sim 4030$  W.

power, however, the relationship does not perform a linear trend. The increasing tendency slows down with the output power, as illustrated in the first run of the laser experiment. Moreover, the temperature of FBGs at the same operation power decreases with the runs of the laser experiment. Compared with the second and third runs of the laser experiment, the temperature of FBGs in the third run is lower, which is contributed by self-annealing of color centers during the lasing process. Different from the thermal annealing process in the UV exposure method, this process is mainly related to the operation power. The thermal slope of HR-FBG and LR-FBG in the third run is  $2.76^\circ\text{C/kW}$  and  $1^\circ\text{C/kW}$ , respectively. Compared with Ref. [24], the temperature characteristic of LR-FBG improves greatly. Lower pulse energy in the fabrication process may generate fewer color centers, and thus the temperature of FBGs increases smoothly with the operation power. A more stable FBG can be realized by further runs of the laser experiment. In this way, a wavelength stable high-power oscillator can be expected, which is meaningful in engineering applications.

Figure 6 shows the stability test of the high-power oscillator at the operation of  $\sim 4030$  W. Figure 6(a) illustrates the power stability test within 1 h. The output power varies near 4030 W in the range of 16 W. No extreme change is observed in the stability test. Figure 6(c) shows the beam quality variation. The beam qualities at times of 10 min, 30 min, and 1 h are experimentally recorded, and the beam profile is relatively stable within the test time. The test results indicate that the oscillator can credibly operate at the 4 kW level.

For the purpose of safety, we test the stability of the oscillator at the operation of the 5 kW level for only  $\sim 42$  s, which is illustrated in Fig. 6(b). The output power is relatively stable within the test time, and the variation is within the range of 7 W.

In order to improve the output power, some optimizations are necessary. Firstly, the configuration of oscillator structure should be optimized, especially the coiling pattern of the YDFs. In this way, the threshold of the SRS effect and TMI effect can be raised up. Secondly, the drawing process of YDFs should be optimized, so that the fiber can endure a higher laser power. Thirdly, a larger mode area fiber can also increase the output power.

#### 4. Conclusion

In conclusion, we fabricate a pair of FBGs using the visible femtosecond laser phase mask scanning technique. Then, a 5-kW-level all-fiber oscillator is constructed using this pair of FBGs. The maximum output laser power is 5027 W, the slope efficiency is 82.1%, and the beam quality factor  $M^2$  is about 1.6 at the maximum. The FBG pair is simply fixed on a water cooling plate without a special package, and the thermal efficiency of HR-FBG and LR-FBG is  $2.76^\circ\text{C/kW}$  and  $1^\circ\text{C/kW}$ , respectively. The research results indicate the reliability of the visible femtosecond laser in fabrication of high-power FBGs, and we present the maximum output power of the oscillator with a core/inner-cladding diameter of 20/400  $\mu\text{m}$ .

## Acknowledgement

This work was supported by the National Natural Science Foundation of China (NSFC) (Nos. 11974427 and 12004431), State Key Laboratory of Pulsed Power Laser (Nos. SKL-2020-ZR05 and SKL2021ZR01), and Postgraduate Scientific Research Innovation Project of Hunan Province (No. CX20200046).

## References

1. D. J. Richardson, J. Nilsson, and W. A. Clarkson, "High power fiber lasers: current status and future perspectives [Invited]," *J. Opt. Soc. Am. B* **27**, B63 (2010).
2. C. Jauregui, J. Limpert, and A. Tünnermann, "High-power fibre lasers," *Nat. Photonics* **7**, 861 (2013).
3. B. Yang, H. Zhang, Q. Ye, H. Pi, C. Shi, R. Tao, X. Wang, and X. Xu, "4.05 kW monolithic fiber laser oscillator based on home-made large mode area fiber Bragg gratings," *Chin. Opt. Lett.* **16**, 031407 (2018).
4. Y. Xiao, F. Brunet, M. Kanskar, M. Faucher, A. Wetter, and N. Holehouse, "1-kilowatt CW all-fiber laser oscillator pumped with wavelength-beam-combined diode stacks," *Opt. Express* **20**, 3296 (2012).
5. H. Yu, X. Wang, R. Tao, P. Zhou, and J. Chen, "1.5 kW, near-diffraction-limited, high-efficiency, single-end-pumped all-fiber-integrated laser oscillator," *Appl. Opt.* **53**, 8055 (2014).
6. B. Yang, H. Zhang, C. Shi, X. Wang, P. Zhou, X. Xu, J. Chen, Z. Liu, and Q. Lu, "Mitigating transverse mode instability in all-fiber laser oscillator and scaling power up to 2.5 kW employing bidirectional-pump scheme," *Opt. Express* **24**, 27828 (2016).
7. B. Yang, H. Zhang, S. Chen, R. Tao, and Q. Lu, "3.05 kW monolithic fiber laser oscillator with simultaneous optimizations of stimulated Raman scattering and transverse mode instability," *J. Opt.* **20**, 025802 (2017).
8. C. A. Robin, I. Hartl, S. Ikoma, H. K. Nguyen, M. Kashiwagi, K. Uchiyama, K. Shima, and D. Tanaka, "3 kW single stage all-fiber Yb-doped single-mode fiber laser for highly reflective and highly thermal conductive materials processing," *Proc. SPIE* **10083**, 100830Y (2017).
9. K. Shima, S. Ikoma, K. Uchiyama, Y. Takubo, M. Kashiwagi, and D. Tanaka, "5-kW single stage all-fiber Yb-doped single-mode fiber laser for materials processing," *Proc. SPIE* **10512**, 105120C (2018).
10. B. Yang, C. Shi, H. Zhang, Q. Ye, H. Pi, R. Tao, X. Wang, P. Ma, J. Leng, Z. Chen, P. Zhou, X. Xu, J. Chen, and Z. Liu, "Monolithic fiber laser oscillator with record high power," *Laser Phys. Lett.* **15**, 075106 (2018).
11. B. Yang, P. Wang, H. Zhang, X. Xi, C. Shi, X. Wang, and X. Xu, "6 kW single mode monolithic fiber laser enabled by effective mitigation of the transverse mode instability," *Opt. Express* **29**, 26366 (2021).
12. Y. Ye, B. Yang, P. Wang, L. Zeng, X. Xi, C. Shi, H. Zhang, X. Wang, P. Zhou, and X. Xu, "Industrial 6 kW high-stability single-stage all-fiber laser oscillator based on conventional large mode area ytterbium-doped fiber," *Laser Phys.* **31**, 035104 (2021).
13. Y. Wang, R. Kitahara, W. Kiyoyama, Y. Shirakura, T. Kurihara, Y. Nakanish, T. Yamamoto, M. Nakayama, S. Ikoma, and K. Shima, "8-kW single-stage all-fiber Yb-doped fiber laser with a BPP of 0.50 mm-mrad," *Proc. SPIE* **11260**, 1126022 (2020).
14. W. Liu, P. Ma, H. Lv, J. Xu, P. Zhou, and Z. Jiang, "General analysis of SRS-limited high-power fiber lasers and design strategy," *Opt. Express* **24**, 26715 (2016).
15. W. Gao, B. Zhao, W. Fan, P. Ju, Y. Zhang, G. Li, Q. Gao, and Z. Li, "Instability transverse mode phase transition of fiber oscillator for extreme power lasers," *Opt. Express* **27**, 22393 (2019).
16. M. Wang, Z. Li, L. Liu, Z. Wang, X. Gu, and X. Xu, "Fabrication of chirped and tilted fiber Bragg gratings on large-mode-area doubled-cladding fibers by phase-mask technique," *Appl. Opt.* **57**, 4376 (2018).
17. K. Jiao, J. Shu, H. Shen, Z. Guan, F. Yang, and R. Zhu, "Fabrication of kW-level chirped and tilted fiber Bragg gratings and filtering of stimulated Raman scattering in high-power CW oscillators," *High Power Laser Sci. Eng.* **7**, e31 (2019).
18. M. Bernier, R. Vallée, B. Morasse, C. Desrosiers, A. Salimonia, and Y. Sheng, "Ytterbium fiber laser based on first-order fiber Bragg gratings written with 400 nm femtosecond pulses and a phase-mask," *Opt. Express* **17**, 18887 (2009).
19. H. Li, X. Zhao, B. Rao, M. Wang, B. Wu, and Z. Wang, "Fabrication and characterization of line-by-line inscribed tilted fiber Bragg gratings using femtosecond laser," *Sensors* **21**, 6237 (2021).
20. L. Lei, H. Li, J. Shi, Q. Hu, X. Zhao, B. Wu, M. Wang, and Z. Wang, "Miniature Fabry-Perot cavity based on fiber Bragg gratings fabricated by fs laser micromachining technique," *Nanomaterials* **11**, 2505 (2021).
21. M. L. Åslund, N. Jovanovic, N. Groothoff, J. Canning, G. D. Marshall, S. D. Jackson, A. Fuerbach, and M. J. Withford, "Optical loss mechanisms in femtosecond laser-written point-by-point fibre Bragg gratings," *Opt. Express* **16**, 14248 (2008).
22. R. J. Williams, N. Jovanovic, G. D. Marshall, G. N. Smith, M. J. Steel, and M. J. Withford, "Optimizing the net reflectivity of point-by-point fiber Bragg gratings: the role of scattering loss," *Opt. Express* **20**, 13451 (2012).
23. R. G. Krämer, C. Matzdorf, A. Liem, V. Bock, W. Middents, T. A. Goebel, M. Heck, D. Richter, T. Schreiber, A. Tünnermann, and S. Nolte, "Femtosecond written fiber Bragg gratings in ytterbium-doped fibers for fiber lasers in the kilowatt regime," *Opt. Lett.* **44**, 723 (2019).
24. R. G. Krämer, F. Möller, C. Matzdorf, T. A. Goebel, M. Strecker, M. Heck, D. Richter, M. Plötner, T. Schreiber, A. Tünnermann, and S. Nolte, "Extremely robust femtosecond written fiber Bragg gratings for an ytterbium-doped fiber oscillator with 5 kW output power," *Opt. Lett.* **45**, 1447 (2020).
25. H. Li, X. Tian, M. Wang, X. Zhao, B. Wu, C. Gao, H. Li, B. Rao, X. Xi, and Z. Wang, "Fabrication of fiber Bragg gratings by visible femtosecond laser for multi-kw fiber oscillator," *IEEE Photon. J.* **14**, 1510904 (2022).
26. C. W. Smelser, D. Grobncic, and S. J. Mihailov, "Generation of pure two-beam interference grating structures in an optical fiber with a femtosecond infrared source and a phase mask," *Opt. Lett.* **29**, 1730 (2004).